Analysis of DNA-Dependent Protein Kinase-Mediated DNA End Joining by Two-Photon Fluorescence Cross-Correlation Spectroscopy

Dennis Merkle,[‡,§,||] Wesley D. Block,[§] Yaping Yu,[§] Susan P. Lees-Miller,*[,§] and David T. Cramb*[,‡]

Department of Chemistry, University of Calgary, 2500 University Drive N.W., Calgary, Alberta, T2N 1N4, Canada, and Cancer Biology Research Group and Department of Biochemistry and Molecular Biology, University of Calgary, 3330 Hospital Drive N.W., Calgary, Alberta, T2N 4N1, Canada

Received November 24, 2005; Revised Manuscript Received January 23, 2006

ABSTRACT: Nonhomologous end joining (NHEJ) is the primary mechanism by which mammalian cells repair DNA double-strand breaks (DSBs). Proteins known to play a role in NHEJ include the DNA-dependent protein kinase catalytic subunit (DNA-PKcs), the Ku 70/Ku 80 heterodimer (Ku), XRCC4, and DNA ligase IV. One of the main roles of the DNA-PKcs−Ku complex is to bring the ends of the DSB together in a process termed synapsis, prior to end joining. Synapsis results in the autophosphorylation of DNA-PKcs, which is required to make the DNA ends available for ligation. Here, we describe a novel assay using two-photon fluorescence cross-correlation spectroscopy that allows for the analysis of DNA synapsis and end joining in solution using purified proteins. We demonstrate that although autophosphorylation-defective DNA-PKcs does not support DNA ligase-mediated DNA end joining, like wild-type (WT) DNA-PKcs, it is capable of Ku-dependent DNA synapsis in solution. Moreover, we show that, in the presence of Ku, both WT DNA-PKcs and autophosphorylation-defective DNA-PKcs promote the formation of multiple, large multi-DNA complexes in solution, suggesting that, rather than align two opposing DNA ends, multiple DNA-PK molecules may serve to bring multiple DNA ends into the NHEJ complex.

DNA double-strand breaks (DSBs)[1] are among the most lethal forms of cellular DNA damage. In mammalian cells, DSBs are repaired predominantly by nonhomologous end joining (NHEJ), a pathway which involves the catalytic subunit of the DNA-dependent protein kinase (DNA-PKcs), the Ku 70/Ku 80 heterodimer (Ku), and the XRCC4/DNA ligase IV complex (reviewed in refs *1* and *2*). Current models for NHEJ predict that the two ends of the DSB are first recognized by the Ku heterodimer. DNA-PKcs is then recruited to DNA-bound Ku to form the DNA-bound DNA-PK complex, and the DNA ends are juxtaposed by the interaction of two molecules of DNA-PK in a process termed synapsis (*3*, *4*). Synapsis results in autophosphorylation of DNA-PKcs, which is thought to be required either to release DNA-PKcs from the DNA ends (*5*, *6*) and/or to remodel the DNA-PK complex such that the DNA ends are made accessible for subsequent ligation by the XRCC4/DNA ligase IV complex (*7*, *8*). Processing of the DNA ends by nucleases such as Artemis (*9*) and possibly other proteins is required for NHEJ, but when this occurs is presently unknown (reviewed in ref *1*).

We and others have identified a total of seven in vitro autophosphorylation sites on DNA-PKcs, six of which are located in the central region of the protein, between amino acids 2609 and 2647 (*10*−*12*). Four of these sites are also phosphorylated in vivo in okadaic-acid-treated cells (threonines 2609, 2638, and 2647 and serine 2612), and threonine 2609 is phosphorylated in vivo in response to ionizing radiation (IR) (*10*, *11*). Cells expressing DNA-PKcs containing serine/threonine to alanine autophosphorylation site mutations at six of these phosphorylation sites (T2609A, S2612A, S2620A, S2624A, T2638A, and T2647A; referred to here as the A6 DNA-PKcs mutant) are extremely radiosensitive (*13*) and are defective in the repair of DNA DSBs in vivo (*8*, *13*). Although the purified A6 mutant protein has protein kinase activity in vitro, it is unable to support DNA end joining by either T4-DNA ligase (*8*) or XRCC4/DNA ligase IV (*7*), suggesting that autophosphorylation at this cluster of sites is required for remodeling of the DNA-PK complex, making the DNA ends accessible for ligation (*14*).

To further investigate the role of DNA-PK and autophosphorylation in NHEJ, we have developed an assay that can detect DNA synapsis and DNA ligation in solution. This assay, which utilizes two-photon excitation fluorescence cross-correlation spectroscopy (TPE-XCS), examines the

* To whom correspondence should be addressed: Department of Chemistry, University of Calgary, 2500 University Drive N.W., Calgary, AB, T2N 1N4, Canada. Telephone: 403-220-8138. Fax: 403-289-9488. E-mail: dcramb@ucalgary.ca.

‡ Department of Chemistry.

§ Cancer Biology Research Group and Department of Biochemistry and Molecular Biology.

|| Present address: Institute of Biophysics, University of Technology Dresden, Tatzberg 47-51, 01307 Dresden, Germany.

[1] Abbreviations: bp, base pair; DNA-PK, DNA-dependent protein kinase holoenzyme; DNA-PKcs, DNA-dependent protein kinase catalytic subunit; ds, double stranded; DSB, double-strand break; DTT, dithiothreitol; Ku, Ku 70/Ku 80 heterodimer; NHEJ, nonhomologous end joining; PAGE, polyacrylamide gel electrophoresis; PMSF, phenylmethyl sulphonyl fluoride; TPE-XCS, two-photon excitation fluorescence cross-correlation spectroscopy; WM, wortmannin; WT, wild type.

10.1021/bi0524060 CCC: $33.50
Published on Web 03/09/2006

interactions between two DNA species bearing spectrally different fluorescent labels and provides information on the concentrations of linked and unlinked species and on their hydrodynamic sizes (*15*, *16*). In TPE-XCS, the time-dependent instantaneous fluorescence intensity from each labeled species is cross-correlated in steps of time, τ. The time dependence (decay) of the XCS signal indicates the loss of the complex from the excitation volume, either by diffusion or dissociation. Thus, it is possible to use TPE-XCS to follow the association of oligonucleotides (labeled with different fluorophores) directly in a reaction mixture. TPE-XCS is complementary to traditional assays in that the reaction solution can be manipulated during observation (i.e., by the addition of proteases). Moreover, TPE-XCS can provide a more detailed examination of heterogeneous mixtures than is possible using only gel-mobility electrophoresis techniques. Because the reactions can be analyzed both with standard electrophoretic mobility shift assays and TPE-XCS, taken together, these two techniques will provide a synergistic examination of biomolecular interactions and thus give more convincing conclusions.

Here, we have used TPE-XCS to examine the role of DNA-PK autophosphorylation and DNA end-joining in solution. Instead of using the XRCC4/DNA ligase IV complex for DNA-PK-mediated DNA end joining, we made use of the fact that, in the presence of catalytically active DNA-PKcs, T4-DNA ligase can form covalently joined end-to-end concatamers of double-stranded (ds) DNA in an ATP-dependent manner (*8*, *17*). Using this assay, we demonstrate that both wild-type (WT) DNA-PKcs and the A6 autophosphorylation site mutant undergo synapsis, that, as demonstrated previously (*8*), the A6 mutant does not support efficient DNA end joining, and that both WT and A6 phosphorylation-defective DNA-PKcs are capable of interacting with multiple DNA ends, producing large multi-DNA−protein complexes in solution.

MATERIALS AND METHODS

Cells. V3 cells expressing DNA-PKcs phosphorylation mutant A6 (T2609A, S2612A, S2620A, S2624A, T2638A, and T2647A) were as previously described (*13*).

Purification and Characterization of Recombinant Human DNA-PKcs Phosphorylation Mutant A6 from V3 Hamster Cells. Recombinant human DNA-PKcs phosphorylation mutant A6 was purified and characterized as described (*8*).

DNA-PK. DNA-PKcs and Ku were purified and characterized from HeLa cells as described (*18*) and stored in 50 mM Tris-HCl at pH 8.0, 5% (v/v) glycerol, 0.2 mM ethylenediaminetetraacetic acid (EDTA), 100 mM KCl, 0.1 mM dithiothreitol (DTT), 0.1 mM benzamidine, 0.5 mM phenylmethyl sulphonyl fluoride (PMSF), and 1 μg/mL pepstatin, in aliquots at −80 °C.

Oligonucleotides. Complementary linear, 61- and 65-base deoxyoligonucleotides were synthesized at The University of Calgary DNA Synthesis Lab. Sequence of strand A: 5′-GCGCAGTCTACAGCGCTGTGGCTCAATTCGCCCTATAGTGAGTCGTATTACAATTCACTGG-3′. Sequence of strand B: 5′-AATTCCAGTGAATTGTAATACGACTCACTATAGGGCGAATTGAGCCACAGCGCTGTAGACTGCGC-3′. Strand A was synthesized with a 5′ amino modification to allowed for fluorescence labeling.

DNA-Strand Annealing, Fluorescence Labeling, and 5′ Overhanging End Phosphorylation. A total of 50 μg each of the 61- and 65-base deoxyoligonucleotides (1 mg/mL stock of each strand) were added to a final volume of 500 μL in 10 mM Tris-HCl at pH 8, 1 mM EDTA, and 50 mM NaCl. The solution was mixed gently and placed in a 90 °C heating block and then left to cool to room temperature over 5 h. This produced 50 μg of a 61-base-pair (bp) dsDNA molecule containing one blunt end that is 5′-amino-modified and one 5′ 4-base overhang. The annealed deoxyoligonucleotide was then phenol/chloroform-extracted and ethanol-precipitated.

A fluorescently labeled group was added to the 5′ amino group of one of the strands using the Alexa Fluor 594 oligonucleotide-labeling kit (Molecular Probes, Eugene, OR) following the recommended procedure of the manufacturer, and the labeled 61-bp dsDNA was gel-purified using the crush-and-soak method (*19*). DNA was quantified at 260 nm in a Beckman DU640 UV spectrometer. The same procedure was followed to generate 50 μg of 61-bp deoxyoligonucleotide labeled with Alexa Fluor 488. Oligonucleotides labeled with Alexa Fluor 594 (red) or Alexa Fluor 488 (green) are referred to as 61R and 61G, respectively.

For some studies, 25 μg each of 61R and 61G was then treated with T4 polynucleotide kinase (Invitrogen, Carlsbad, CA) following the recommended procedure of the manufacturer, to produce 61R and 61G oligonucleotides that contained the fluorescence label on the 5′ blunt end and a phosphorylated 5′ overhanging end. Phosphorylated 61R and 61G oligonucleotides are referred to as 61R-P and 61G-P, respectively.

DNA End-Joining Assays. Oligonucleotides 61R-P and 61G-P (at the amounts indicated) were incubated with 0.5 unit of T4-DNA ligase (Invitrogen, Carlsbad, CA) in ligation buffer [50 mM Tris-HCl at pH 7.5, 10 mM $MgCl_2$, 75 mM KCl, 1 mM DTT, 1 mM ATP, and 5% (w/v) PEG-8000] for 30 min at room temperature in a total volume of 10 μL. Where indicated, reactions also contained purified DNA-PKcs (WT or autophosphorylation mutant A6) and/or Ku (at the amounts indicated). Wortmannin (WM, Sigma Chemical Co.) was added to 400 nM where indicated. Reaction products were deproteinated by the addition of proteinase K (Life Technologies, Inc.) to a final concentration of 2 mg/mL and incubated for 30 min at 37 °C. DNA was resolved by electrophoresis on a nondenaturing 12% polyacrylamide gel in Tris-glycine buffer (50 mM Tris and 0.38 M glycine at pH 8.0). Images were generated and recorded using a GelDoc fluorescence detector (BioRad). Reactions analyzed using TPE-FCS and TPE-XCS were performed under the same conditions as above and subsequently diluted to a final volume of 75 μL in 50 mM Tris-HCl at pH 7.5 containing 75 mM KCl and delivered into a 500 μL glass sample chamber (University of Calgary glass shop).

DNA Synapsis Assays. Oligonucleotides 61R and 61G were incubated with DNA-PKcs and/or Ku (at the amounts indicated) in DNA-binding buffer [25 mM Tris-HCl at pH 7.5, 50 mM KCl, 10% (v/v) glycerol, and 2 mM DTT] for 15 min at room temperature in a total volume of 10 μL. Where indicated, reactions were treated with 2.5 mM bis-(sulfosuccinimydyl) suberate (BS^3) cross-linker (Pierce, Rockford, IL) for 10 min at room temperature as described previously (*20*). DNA−protein complexes were analyzed

using TPE-XCS and/or resolved by electrophoresis on 0.7% agarose gels, and images were generated as described above.

FCS/XCS Experimental Setup. Samples were excited using 780 nm, 100 fs laser light from a Spectra Physics Tsunami laser operating at 82 MHz. The laser power was attenuated to 30 mW with a neutral density filter to avoid photobleaching. Alexa-fluor 594 and 488 both have appreciable two-photon excitation probability at 780 nm. The laser beam was expanded using a Galilean telescope to slightly overfill the back aperture of a 40×, 0.9 NA Zeiss objective lens mounted on a Zeiss Axiovert 200 fluorescence microscope. TPE fluorescence was collected by the same objective lens, passed through a broad band-pass filter to remove laser light (Omega Optical, XF3100), and reflected off a dichroic optic (Chroma, 700DCSPXR) and through a tube lens in the side port of the microscope. The fluorescence then encounters a second dichroic optic (Chroma 565DCLP) to separate the red and green light. The spectrally separated light passes through band-pass filters (Chroma, E590LPv2 and D535/50x for the red and green emission, respectively) and is coupled into optical fibers located at the focus of the tube lens. Using the optical fibers, the fluorescence is detected by two Si avalanche photodiodes (APDs, Perkin−Elmer, SPCQ-200). The output of the APDs was analyzed using a correlator card (ALV-5000, Langen, Germany) installed in a PC computer.

FCS and XCS Data Analysis. Autocorrelation decays could be modeled assuming a Gaussian TPE volume using the following equation (*15*)

$$G(\tau) = \frac{1}{(\sum \eta_k N_k)^2} \sum_i \eta_i^2 N_i \left(1 + \frac{8D_i\tau}{r_0^2}\right)^{-1} \left(1 + \frac{8D_i\tau}{z_0^2}\right)^{-1/2} \quad (1a)$$

$$G(\tau) = G(0) \sum_i \left(1 + \frac{8D_i\tau}{r_0^2}\right)^{-1} \left(1 + \frac{8D_i\tau}{z_0^2}\right)^{-1/2} \quad (1b)$$

where the subscript i indicates different labeled species, τ is the lagtime, η is the count rate per diffusing species, N is the average number of diffusing species in the excitation volume, D is the diffusion constant, r_0 is the laser beam radius at its focus, and z_0 is the depth of focus. The TPE excitation volume was calibrated by measuring the ACF for a 100 nM solution of rhodamine 6G ($D = 2.8 \times 10^{-10}$ m^2/s) in 50 mM Tris-HCl at pH 8.0. The excitation volume was found to be 1.16 fL.

Cross-correlation decays can be modeled as above using the following equation (*15*)

$$G_{ij}(\tau) = \frac{1}{(\sum \eta_i N_i)(\sum \eta_j N_j)} \sum \eta_i \eta_j N_{ij} \left(1 + \frac{8D_{ij}\tau}{r_0^2}\right)^{-1} \times \left(1 + \frac{8D_{ij}\tau}{z_0^2}\right)^{-1/2} \quad (2a)$$

$$G_{ij}(\tau) = G_X(0) \sum_{ij} \left(1 + \frac{8D_{ij}\tau}{r_0^2}\right)^{-1} \left(1 + \frac{8D_{ij}\tau}{z_0^2}\right)^{-1/2} \quad (2b)$$

where the subscripts i, j, and ij represent red-labeled, green-labeled, and dual-color-labeled diffusing species, respectively. Nonlinear least-squares fitting to the data was accomplished using the software package, Origin.

In our study, we mix equal concentrations of red- and green-labeled oligonucleotides and assess their ligation or synapsis. If we consider that only pairs of oligonucleotides can be ligated, then there will be the following types of species in solution: red−green (×2), red−red, green−green, red, and green. Within a reasonable approximation (i.e., no quenching or energy transfer), the red−red- and green−green-ligated oligonucleotides will have twice the brightness as the other species in solution. The concentrations of species in solution can be determined from the correlation amplitudes also known as $G(0)$ values. From eqs 1b and 2b, we can develop the relations for the autocorrelation amplitudes and cross-correlation amplitude.

For the red channel,

$$G_r(0) = \frac{(2\eta_r)^2 C_{2r} + \eta_r^2 C_r + \eta_r^2 C_{rg}}{N_A V_{eff} (2\eta_r C_{2r} + \eta_r C_r + \eta_r C_{rg})^2} \quad (3)$$

where C_{2r}, C_r, and C_{rg} are the concentrations of red−red-ligated oligonucleotides ($C = N/V_{eff}$), red-free oligonucleotides, and red−green-ligated oligonucleotides, respectively. N_A is Avogadro's number, and V_{eff} is the effective $1/e^2$ two-photon excitation volume and is equal to $(\pi/2)^{3/2} r_0^2 z_0$. The brightness, η_r, can be factored out of this equation, and the terms can be gathered to give the following equation

$$G_r(0) = \frac{2C_{2r} + C_{rtot}}{N_A V_{eff} C_{rtot}^2} \quad (4)$$

where we define $C_{rtot} = 2C_{2r} + C_r + C_{rg}$.

Similarly, we can develop a relation for $G_g(0)$, which is analogous to eq 4

$$G_g(0) = \frac{2C_{2g} + C_{gtot}}{N_A V_{eff} C_{gtot}^2} \quad (5)$$

where we define $C_{gtot} = 2C_{2g} + C_g + C_{rg}$.

For the cross-correlation amplitude, we find that the following relation emerges:

$$G_X(0) = \frac{\eta_r \eta_g C_{rg}}{N_A V_{eff} (2\eta_r C_{2r} + \eta_r C_r + \eta_r C_{rg})(2\eta_g C_{2g} + \eta_g C_g + \eta_g C_{rg})} \quad (6)$$

Again, gathering terms and simplifying reveals the following equation

$$G_X(0) = \frac{C_{rg}}{N_A V_{eff} C_{rtot} C_{gtot}} \quad (7)$$

The dependence on the effective volume can be eliminated by taking the ratio of the cross-correlation amplitude to the autocorrelation amplitudes

$$\frac{G_X(0)}{N_A V_{eff} G_r(0) G_g(0)} = \frac{C_{rg}}{\frac{(2C_{2r} + C_{rtot})(2C_{2g} + C_{gtot})}{C_{rtot} C_{gtot}}} \quad (8)$$

If we assume that there is no dependence of the ligation on the fluorescence label, then for equimolar mixtures of red and green oligonucleotides, one has $C_{2r} = C_{2g}$, $C_{rtot} = C_{gtot}$, and $C_{2r} = C_{rg}/2$. This allows eq 8 to be simplified

$$\frac{G_X(0)}{N_A V_{eff} G_r(0) G_g(0)} = \frac{C_{rg} C_{rtot}^2}{(C_{rg} + C_{rtot})^2} \quad (9)$$

Because the correlation amplitudes can be all measured and C_{rtot} is known, C_{rg} can be determined using the above equation.

RESULTS

Development of an "In-Solution" DNA End-Joining Assay. To examine the role of DNA-PKcs autophosphorylation in DNA end joining and synapsis, we generated two sets of dsDNA oligonucleotides, referred to as 61R-P and 61G-P, and 61R and 61G, where R and G represent a unique fluorescent dye attached to the 5′ end of one of the strands of the dsDNA oligonucleotide and P represents the 5′-phosphorylated form of the oligonucleotide (see the Materials and Methods for details). Because 61R-P and 61G-P each contained a 5′ fluorophore at the blunt end and a 5′-phosphorylated group at the opposite end, they can be ligated to produce oligonucleotide dimers but not multimers. In contrast, oligonucleoptides 61R and 61G do not contain a 5′-phosphate group and cannot be ligated.

We first examined the ability of T4-DNA ligase to support the ligation of 61R-P and 61G-P using a gel-based assay. The fluorescently labeled oligonucleotides were preincubated in the absence or presence of T4-DNA ligase and resolved by nondenaturing polyacrylamide gel electrophoresis (PAGE). Incubation of 61R-P or 61G-P with T4-DNA ligase resulted in a slower migration of the fluorescently labeled DNA species, which was consistent with the formation of a DNA dimer (apparent size of approximately 120 bp) (lane 2 in Figure 1). As expected, T4-DNA ligase was unable to support the ligation of the nonphosphorylated oligonucleotides 61R and 61G (lane 3 in Figure 1). As shown previously (*8*), T4-DNA ligase-mediated end joining occurred in the presence of Ku alone (lane 4 in Figure 1). Also, as shown previously (*8*, *17*), the protein kinase activity of DNA-PKcs was required for DNA-PK-dependent, T4-DNA ligase-mediated, end-to-end joining of dsDNA oligonucleotides, because the DNA-PK inhibitor, WM, prevented T4-DNA ligase-mediated ligation in the presence of DNA-PKcs (lane 6 in Figure 1). WM had no effect on T4-DNA ligase-mediated joining either in the absence or presence of Ku (*8*). The treatment of the samples with proteinase K did not alter the migration of the fluorescent species, indicating that the shift in migration was not due to protein binding (data not shown). As shown previously (*8*), the A6 autophosphorylation mutant was defective in T4-DNA ligase-mediated end joining compared to WT DNA-PKcs (lane 8 in Figure 1).

Next, a mixture (50% 61R-P and 50% 61R-P) of labeled DNA oligonucleotides was preincubated with T4-DNA ligase under identical conditions, and the products were analyzed using TPE-XCS. As shown in the gel-based assay (lane 2 in Figure 1), the reaction conditions used resulted in virtually complete ligation of the DNA; therefore, approximately 50% of the total DNA present would be predicted to contribute

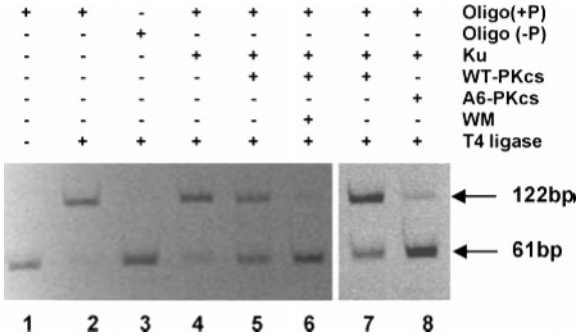

FIGURE 1: Autophosphorylation-defective DNA-PKcs does not support the ligation of DNA ends. Fluorescently labeled dsDNA oligonucleotides were incubated with T4-DNA ligase and or purified DNA-PKcs and Ku as indicated, and the products were analyzed by nondenaturing PAGE. Lanes 1, 2, and 4−6 contained 62.5 ng (1.5 pmol) of 61R-P dsDNA oligonucleotide [Oligo (+P)]. Lane 3 contained 62.5 ng of 61R oligonucleotide [Oligo (−P)]. Lanes 7 and 8 contained 125 ng (3 pmol) of 61G-P oligonucleotide. Lanes 2−8 contained 0.5 units of T4-DNA ligase. Lanes 4−6 contained 0.45 μg (3 pmol) of purified human Ku heterodimer. Lanes 7 and 8 contained 0.9 μg (6 pmol) of purified human Ku heterodimer. Lanes 5 and 6 contained 3 μg (6 pmol) of purified human (HeLa cell) DNA-PKcs. In lane 6, DNA-PKcs was pretreated with 400 nM WM prior to the addition to end-joining assays. Lane 7 contained 6 μg (12 pmol) of WT DNA-PKcs purified from V3 cells transfected with cDNA for human DNA-PKcs. Lane 8 contained 6 μg of autophosphorylation-defective DNA-PKcs mutant purified from V3 cells as described (*8*). The positions of the 61-bp monomer and the 122-bp dimer are indicated by the arrows.

to a cross-correlation signal. Typical correlation decay spectra for this reaction are shown in Figure 2. When the data was fitted and the concentration of cross-correlating species, C_{rg}, was calculated [using eq 9 and the values $C_{rtot} = 160$ nM, $G_X(0) = 0.0055$, and $G_r(0) = G_g(0) = 0.015$] approximately as 75 nM of the DNA. Because the total amount of DNA was 160 nM (see the caption to Figure 2) and a maximum of 50% can contribute to the cross-correlation (i.e., 80 nM), this value agrees well with the value anticipated from the gel reaction. As expected from the results shown in Figure 1, no cross-correlation was observed when 61R-P and 61G-P were incubated in the absence of T4-DNA ligase or when the unphosphorylated oligonucleotides (61R and 61G) were incubated with T4-DNA ligase (data not shown).

Autophosphorylation-Defective DNA-PKcs Does Not Support Ligation of DNA Ends. We next used the TPE-XCS assay to examine the effect of DNA-PK autophosphorylation on DNA end joining in solution. Cross-correlation was observed in TPE-XCS when WT DNA-PKcs was incubated with Ku and T4-DNA ligase (Figure 3A), indicating that these conditions support DNA end joining. Fitting of these data produced a total cross-correlated DNA concentration of 36 nM [$C_{rtot} = 160$ nM, $G_X(0) = 0.005$, $G_r(0) = C_g(0) = 0.017$], which is reasonable because not all 100% of the DNA was ligated under these conditions (lanes 5 and 7 in Figure 1), and therefore, we would expect to see less than 50% of the total DNA (160 nM) contribute to a cross-correlation. In contrast, no cross-correlation was observed when reactions contained autophosphorylation-defective DNA-PKcs mutant, A6 (Figure 3C). This result, using TPE-XCS, is therefore in keeping with the results shown in lane 8 in Figure 1 and those previously reported (*8*) and confirms that the A6 mutant does not support DNA end joining by T4-DNA ligase.

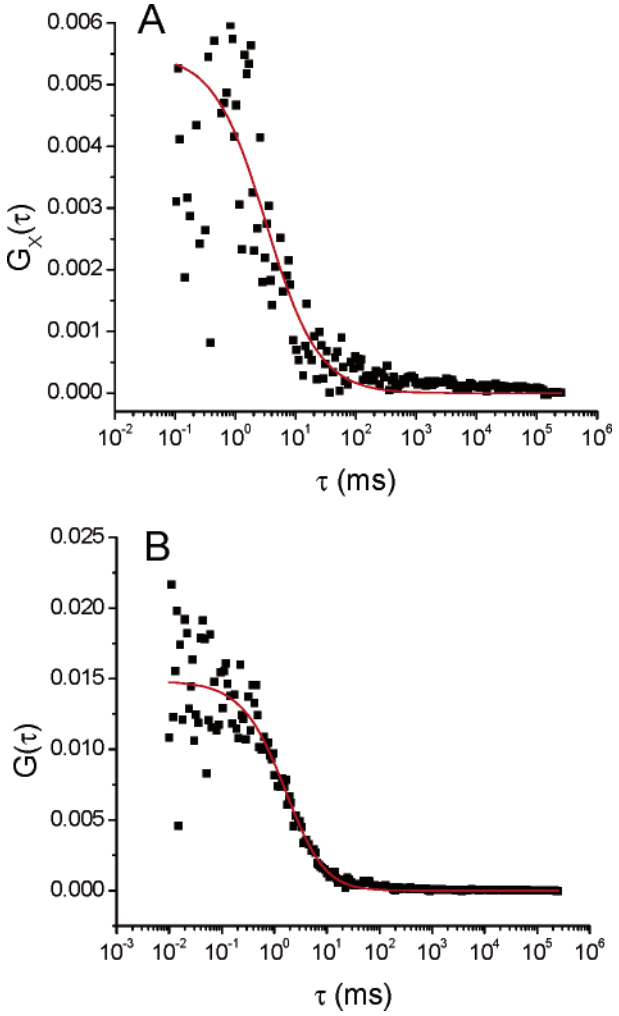

FIGURE 2: Correlation decay curves demonstrating T4-mediated ligation in solution. The solution contained a mixture of 250 ng of 61R-P, 250 ng of 61G-P (12 pmol total), and 1 unit of T4-DNA ligase. A depicts the measured cross-correlation data (■) and fit using eq 2b (red line). B depicts the measured autocorrelation for the red-detection channel (■) and fit using eq 1b (red line).

DNA-PKcs Supports Dynamic Synapsis of Multiple DNA Ends. We next employed the same conditions to examine the role of DNA-PK in synapsis of DNA ends. The first step in synapsis is said to occur when two opposing DNA ends are brought together by DNA-bound DNA-PK molecules (*3*, *4*, *17*). Synapsis was originally demonstrated by the ability of a dsDNA oligonucleotide (coupled to neutravidin-agarose beads) to pull down radioactively labeled dsDNA oligonucleotides (*3*). The addition of DNA-PKcs alone or in combination with Ku, resulted in radioactively labeled DNA being precipitated with the immobilized DNA, indicating that DNA-bound DNA-PKcs alone or in complex with Ku can bring opposing ends of the DSB together (*3*). One of the advantages of TPE-XCS is that the synaptic reaction can be studied in solution without the need for DNA-conjugated agarose beads and the potential for nonspecific protein interactions with the beads. For the TPE-XCS assays, we used nonphosphorylated oligonucleotides (61R and 61G) that cannot be ligated (see the Materials and Methods and lane 3 in Figure 1). This ensured that any cross-correlation signal observed was due to synapsis and not to ligation. We and others have observed that the interaction between DNA-PKcs and Ku on small ds oligonucleotides is weak and/or transient and that chemical cross-linkers are required to stabilize the interaction of DNA-PKcs−Ku with DNA in vitro (*7*, *13*, *20*). Therefore, we have compared solutions without and with the chemical cross-linker BS^3. Those reactions with BS^3 were treated as described previously (*20*). When purified Ku heterodimer was incubated with the nonligatable oligonucleotides, no cross-correlation was detected (Figure 4A), indicating that, even in the presence of BS^3, Ku molecules

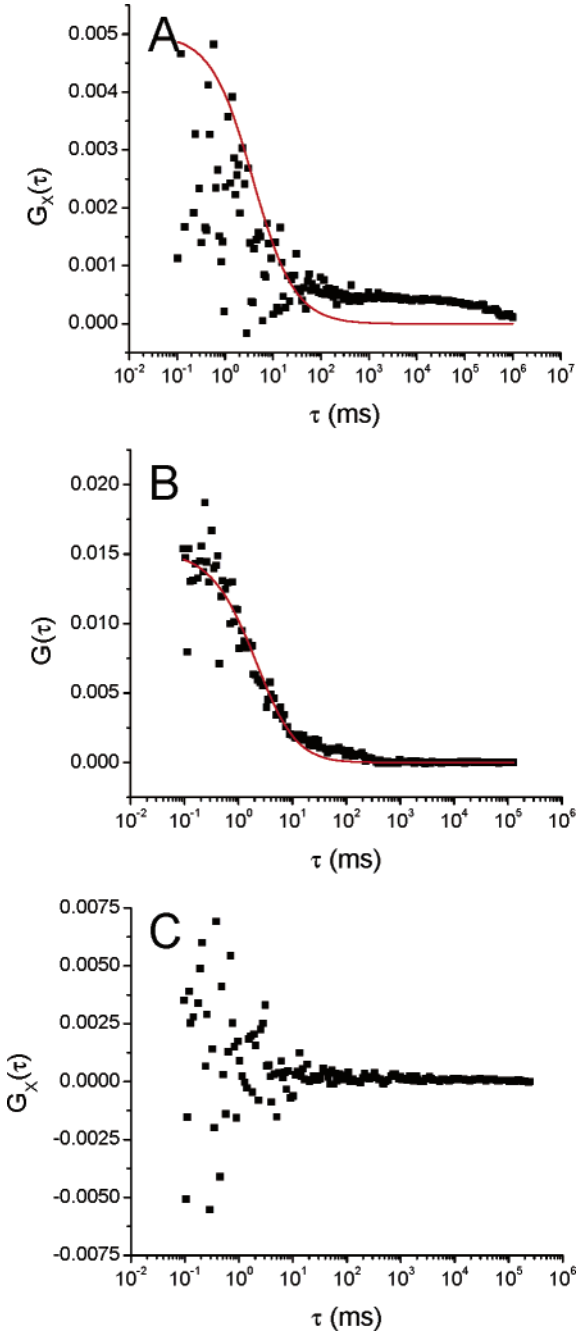

FIGURE 3: Correlation decay curves demonstrating that autophosphorylation-defective DNA-PKcs does not support the ligation of DNA ends. A−C contained a mixture of 250 ng of 61R-P, 250 ng of 61G-P (12 pmol total), and 1 unit of T4-DNA ligase. A and B also contained 3.6 μg (~24 pmol) of purified human Ku heterodimer and 24 μg (51 pmol) of purified human DNA-PKcs. C also contained 24 μg of purified A6 DNA-PKcs mutant. Experimental cross-correlation (■, A and C) and autocorrelation data (■, B) were fit using eqs 2b and 1b, respectively (red lines).

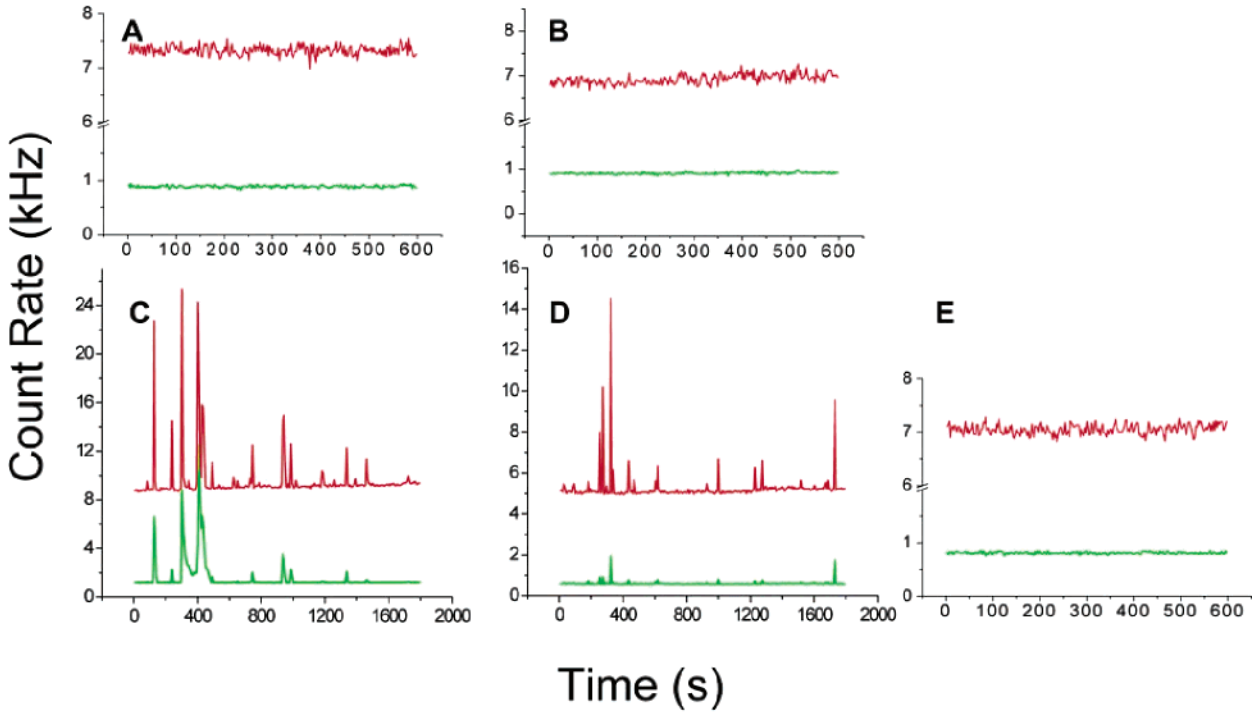

FIGURE 4: DNA-PKcs is capable of synapsing multiple DNA ends in the presence of Ku. Reactions containing nonligatable, fluorescently labeled oligonucleotides plus purified proteins as indicated were examined by TPE-XCS. Count rate trajectories are shown, where green represents the 61G signal and red represents the 61R signal. All reactions contained 250 ng of both 61R and 61G oligonucleotides (11 pmol total) and were treated with 2.5 mM BS^3 cross-linker for 10 min prior to analysis by TPE-XCS (see the Methods and Materials). (A) A 10 min count rate trajectory of a reaction containing only 60R, 61G, and Ku. (B) A 10 min count rate trajectory of a reaction containing 5 μg (11 pmol) of purified WT DNA-PKcs but no Ku. (C) A 30 min count rate trajectory of a reaction containing Ku plus 5 μg (11 pmol) of purified WT DNA-PKcs. (D) A 30 min count rate trajectory of a reaction containing Ku plus 5 μg of purified A6 mutant DNA-PKcs. (E) A 10 min count rate trajectory of the sample in C, after treatment with proteinase K.

bound to the ends of short dsDNA oligonucleotides do not interact with other DNA end-bound Ku molecules; i.e., the DNA-bound Ku molecules do not undergo synapsis. Similarly, when WT DNA-PKcs was incubated with the nonligatable ds oligoucleotides, even in the presence of BS^3, no cross-correlation and therefore no synapsis was observed (Figure 4B). One interpretation of this result is that, consistent with our previous findings in gel-based assays (*7*, *13*, *20*), DNA-PKcs does not form a stable interaction with short dsDNA oligonucleotides even in the presence of the cross-linker. Alternatively or in addition, the results could indicate that DNA-PKcs−DNA molecules do not support synapsis with other DNA-bound DNA-PKcs molecules. Significantly, when WT DNA-PKcs was incubated with Ku and DNA, multiple fluorescence intensity spikes occurred simultaneously in both detection channels, indicating that, in the presence of DNA-PKcs and Ku, several DNA molecules were being brought together in solution (Figure 4C). We interpret these data to indicate that the DNA-PK holoenzyme (i.e., DNA + Ku + DNA-PKcs) supports synapsis. Control experiments where 61R and 61G were mixed solely with BS^3 produced no evidence of synapsis. Coincident intensity spikes were not observed when DNA-PKcs−Ku−DNA reactions were treated with proteinase K prior to TPE-XCS (Figure 4E), showing that multi-DNA complexes and hence synapsis was protein-mediated. When the autophosphorylation-defective mutant A6 DNA-PKcs was incubated with Ku and the unligatable, fluorescently labeled oligonucleotides, again, coincident intensity spikes were observed (Figure 4D), indicating that the A6 mutant, like the WT, is capable of undergoing synapsis. Electrophoretic mobility shift assays of the solutions producing the large complexes indicate that greater than 90% of the material is found in these complexes (data not shown).

Although the data show clear evidence for coincident intensity spikes when DNA-PKcs (the WT or phosphorylation mutant) were incubated with Ku and dsDNA, the count rate trajectories displayed a very heterogeneous size distribution of DNA−protein complexes, resulting in cross-correlation decay curves, which were difficult to analyze (data not shown). As a result, we applied shorter data collection times to select for a more consistent distribution in the fluorescence intensity spiking. This produced a clear cross-correlation for DNA with Ku and either WT DNA-PKcs (Figure 5A) or A6 mutant DNA-PKcs (Figure 5B). The insets in Figure 5 display count rate trajectories for each respective run. While these cross-correlation decay curves directly demonstrate complexes containing multiple green- and red-labeled DNA molecules, the heterogeneity of the fluorescence intensity spikes makes the decays difficult to quantify and, therefore, interpretation of the $G(0)$ values in terms of complex concentrations is not warranted. We observed 71 such count rate intensity peaks in a total of 62 min of data collection for the reaction containing Ku−DNA and WT DNA-PKcs (1.15 multiple DNA−protein complexes diffusing through the excitation volume per minute), and we observed 70 peaks in a total of 60 min of data collection for the reaction containing Ku−DNA and A6 mutant DNA-PKcs (1.17 multiple DNA−protein complexes diffusing through the excitation volume per minute), demonstrating that both A6

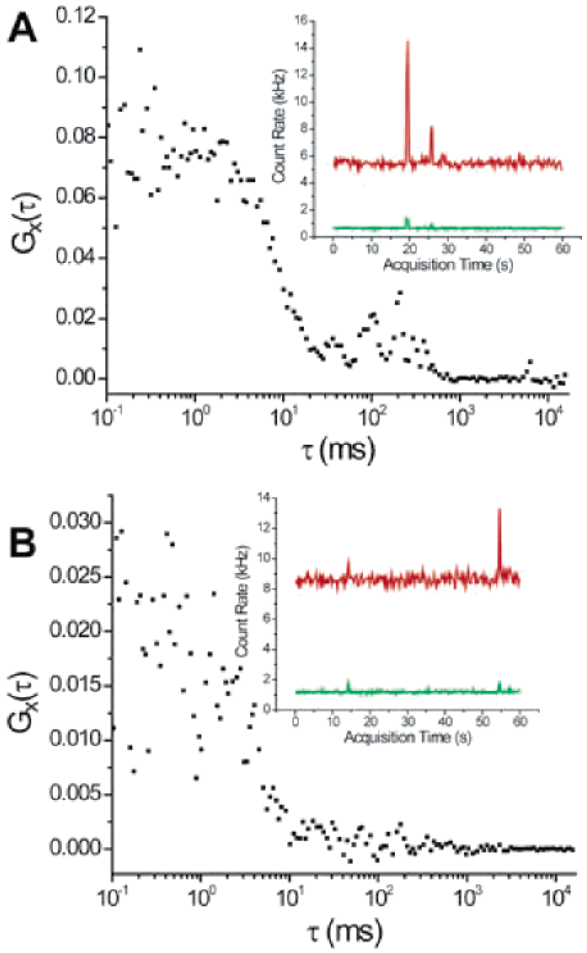

FIGURE 5: Cross-correlation decay curves (G_X) indicating that synapsis involves multiple green and red DNA molecules. (A) Cross-correlation decay for a 1 min data collection of the same reaction outlined in Figure 3A. (B) Cross-correlation decay for a 1 min data collection of the same reaction outlined in Figure 3C. Black squares represent experimental data. Insets indicate count rate trajectories for each respective run. Green represents the 61G signal, and red represents the 61R signal.

and WT DNA-PKcs have a similar affinity for other DNA-PK holoenzymes. The treatment of the samples with proteinase K abolished all cross-correlation decays and any count rate trajectory intensity spiking, indicating that the multi-DNA complexes were protein-mediated (data not shown).

Reactions performed in the absence of the BS^3 cross-linker produced similar results, except that the intensity spikes were not as frequent (Figure 6). For example, in a reaction containing Ku−DNA and WT DNA-PKcs, in the absence of the cross-linker, four fluorescence intensity peaks were observed in a total of 20 min of data collection (0.2 multiple DNA−protein complexes per minute). These results suggest that the simultaneous interactions of multiple DNA molecules is DNA-PK-mediated and may be transient, because cross-linking the proteins results in a stabilization of and subsequent increase in frequency of these complexes. We note that there is some evidence of photobleaching in the red channel in Figure 6A. A cross-correlation decay obtained from this solution (Figure 6B) indicates that there are also many smaller synapsed holoenzymes present. According to eq 2, if only the large complexes and nonsynapsed oligonucleotides contributed to $G_X(\tau)$, then the value of the

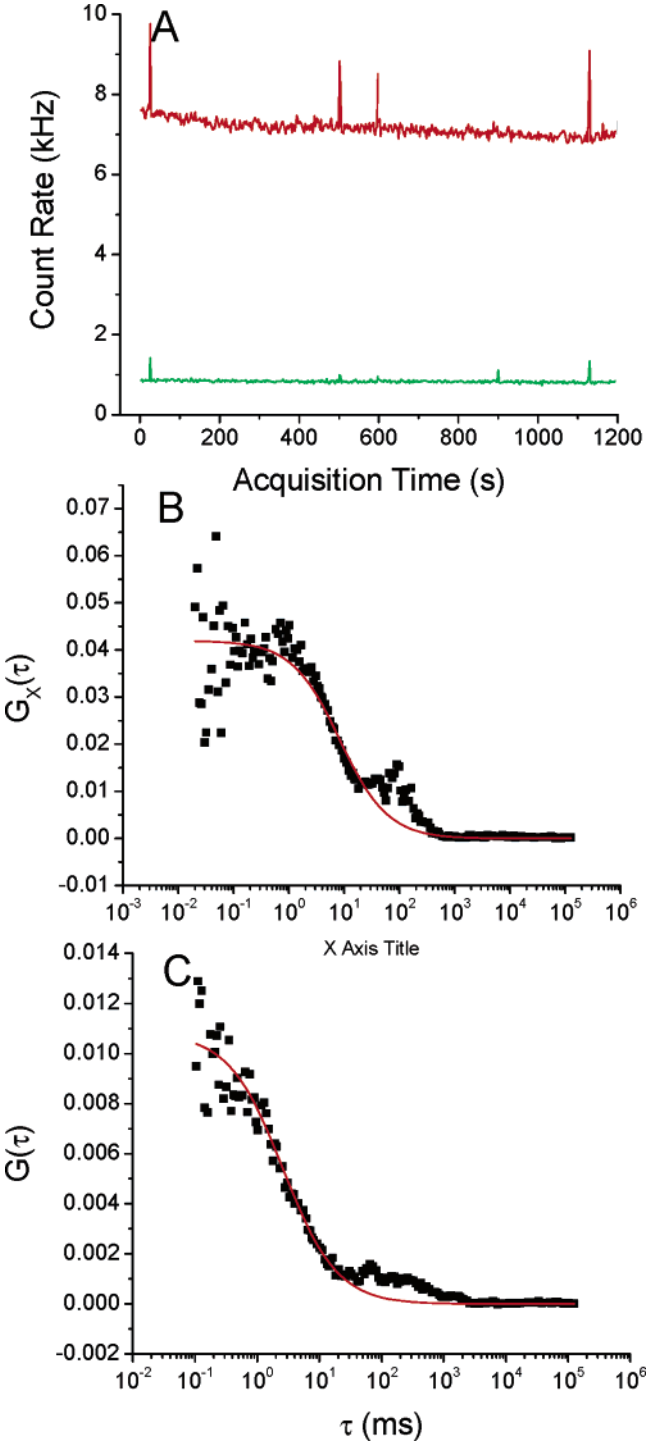

FIGURE 6: Synapsis in the absence of the cross-linker, BS^3. The solution contained 250 ng of both 61R and 61G oligonucleotides (11 pmol total), 1.75 μg Ku (11 pmol), plus 5 μg (11 pmol) of purified WT DNA-PKcs. A shows a 20 min long count rate trajectory. The red and green traces represent the intensities from the red (61R) and green (61G) detection channels, respectively. Note that there are fewer large complexes (intensity spikes) than in Figure 5. B contains the fluorescence cross-correlation decay (■) and fit using eq 2b (red line). C contains the fluorescence autocorrelation decay for the red channel (61R, ■) and fit using eq 1b (red line).

amplitude [$G_X(0)$] can be estimated at approximately 0.011 (the measured value is 0.04). The estimate was calculated using $N_i = N_j = 150$, $\eta_i = 0.08$ kHz/molecule, and $\eta_j = 0.01$ kHz/molecule for the free species and $N_{ij} = 0.01$, $\eta_i =$

10 kHz/complex, and $\eta_j = 1.5$ kHz/complex for the synapsed species. With fewer single oligonucleotides in solution (i.e., those lost to synapsis), the value of $G_X(0)$ would increase from the predicted 0.011. If we considered a scenario where all species in solution are undergoing pairwise synapsis, $G_X(0)$ is calculated to be 0.035. This estimate was made using the above values for larger complexes and assuming that the bulk of the oligonucleotides is associated in pairs. Thus, in solution, one would observe $N'_{ij} = 75$ 61R−61G species/TPE volume and 37.5 61R−61R and 61G−61G species/TPE volume. Interestingly, the autocorrelation amplitudes are fairly insensitive to these two scenarios. $G_R(0)$ values (red channel) are calculated to be 0.013 for only large complexes and unbound oligonucleotides and 0.014 for large complexes with all pairwise-bound oligonucleotides. Both are close to the measured value, 0.012 (Figure 6C). Thus, it would appear that there is a background level of synapsis in the non-BS^3-treated WT DNA-PK reaction.

DISCUSSION

Here, we describe a new method (TPE-XCS) for detecting and measuring the ability of proteins to mediate protein−DNA interactions in solution. Using fluorescently labeled dsDNA oligonucleotides that either contained or lacked a 5′-phosphate group, we were able to distinguish between protein-mediated DNA ligation and synapsis, two important steps in the NHEJ pathway.

TPE-XCS and FCS data were fitted using eqs 1b and 2b, as appropriate (see Figures 2, 3, and 6). The calculated decays represent the data reasonably well, but the deviations are worth discussing. First, some of the decays display long tails, which can be rationalized as minor slow changes in fluorescent-label concentrations. This results from some of the longer run times used here, where slow photobleaching and/or minor solvent evaporation can take place. This behavior was not included in the model equations (1b and 2b), and thus, the calculated decays do not match well the long lagtime ($\tau > 10^2$ ms) portion of the data. This does not significantly affect the interpretation of the $G(0)$ values, which were used to quantify the amount of associated oligonucleotides, because the count rate trajectories changed only by a few percent over the long runs (up to 20 min). Given the scatter in the data, $G(0)$ values are estimated to have 15% error. We also note the appearance of a bump in the decays at around 10^2 ms (parts B and C of Figure 6). This artifact occurs only when large, bright slow-moving complexes are observed in the count rate trajectories. We have previously attributed this to ~60 Hz line noise in the laser power supply, which manifests in the correlation decays (*16*).

Using TPE-XCS, we provide further evidence that one DNA-bound DNA-PK (i.e., DNA + Ku + DNA-PKcs) molecule can interact with other DNA-bound DNA-PK molecules, i.e., undergo synapsis. Our results are in agreement with those of Chu and colleagues (*3*), except that, under the conditions used in this study, DNA-PKcs alone did not support synapsis of DNA ends, even in the presence of the BS^3 cross-linker and under similar salt conditions to those used previously (*3*). Experiments in which DNA-PKcs mediated synapsis were observed by electron and atomic force microscopy generally used linear of DNA of several kilobases, which has the flexibility to loop around (*3*, *6*, *21*, *22*). In contrast, our study used small oligonucleotides in which only one end of the DNA was available for binding, perhaps accounting for this difference in the results.

Our results also confirm our previous studies, demonstrating the inability of the autophosphorylation-defective DNA-PKcs mutant protein (A6) to support DNA end joining (*7*, *8*). Moreover, using TPE-XCS, we show that, like WT DNA-PKcs, autophosphorylation-defective DNA-PKcs (A6 mutant), in the presence of Ku, is capable of synapsis (Figure 4D).

Significantly, using both WT and autophosphorylation-defective DNA-PKcs proteins, complexes of a variety of different sizes containing multiple DNA molecules were observed (parts C and D of Figure 4). The multi-DNA−protein complexes were protein-mediated, because the addition of proteinase K to the reactions abolished all count rate trajectory intensity spiking and cross-correlation signals (Figure 4E). Together, these results suggest that multiple DNA-PKcs−Ku−DNA molecules can interact in solution to form multiple protein−DNA complexes of heterogeneous size and that these interactions are mediated by DNA-PKcs and may be transient, because cross-linking the proteins results in a stabilization of and subsequent increase in frequency of these complexes. In addition, these data suggest that once the DNA-PK holoenzyme (DNA-PKcs and Ku plus DNA) is formed, the complex has a high affinity for other DNA−DNA-PKcs−Ku complexes. These observations are consistent with our previous paper on the formation of large, DNA-PK-mediated protein−DNA complexes containing multiple DNA molecules as detected using electron spectroscopic imaging (ESI) (*6*). On the basis of these studies, we propose that DNA-PK may have the ability to bring together multiple DNA molecules in multiprotein−multi-DNA-containing complexes rather than simply support one-to-one DNA end joining as previously proposed.

ACKNOWLEDGMENT

We thank Dr. Katheryn Meek (Michigan State University) for V3 cells expressing the DNA-PKcs autophosphorylation mutant A6 (also called ABCDE) and Donna Boland of the Southern Alberta Hybridoma Facility for growing the V3 cells. This work was supported by Grant 13639 from the Canadian Institutes of Health Research (to S. P. L.-M.) and by the Canadian Institute for Photonics Innovation (to D. T. C.). D. M. was supported by a graduate studentship from the Alberta Cancer Foundation. W. D. B. was supported by graduate studentships from the Alberta Heritage Foundation for Medical Research (AHFMR) and the Natural Sciences and Engineering Research Council of Canada (NSERC). S. P. L.-M. is a Scientist of the AHFMR, an Investigator of the Canadian Institutes for Health Research, and holds the Alberta Cancer Foundation/Engineered Air Chair in Cancer Research.

REFERENCES

1. Lees-Miller, S. P., and Meek, K. (2003) Repair of DNA double strand breaks by non-homologous end joining, *Biochimie 85*, 1161−1173.
2. Lieber, M. R., Ma, Y., Pannicke, U., and Schwarz, K. (2003) Mechanism and regulation of human non-homologous DNA end-joining, *Nat. Rev. Mol. Cell. Biol. 4*, 712−720.

3. DeFazio, L. G., Stansel, R. M., Griffith, J. D., and Chu, G. (2002) Synapsis of DNA ends by DNA-dependent protein kinase, *EMBO J. 21*, 3192−3200.
4. Weterings, E., and van Gent, D. C. (2004) The mechanism of non-homologous end-joining: A synopsis of synapsis, *DNA Repair 3*, 1425−1435.
5. Chan, D. W., and Lees-Miller, S. P. (1996) The DNA-dependent protein kinase is inactivated by autophosphorylation of the catalytic subunit, *J. Biol. Chem. 271*, 8936−8941.
6. Merkle, D., Douglas, P., Moorhead, G. B., Leonenko, Z., Yu, Y., Cramb, D., Bazett-Jones, D. P., and Lees-Miller, S. P. (2002) The DNA-dependent protein kinase interacts with DNA to form a protein−DNA complex that is disrupted by phosphorylation, *Biochemistry 41*, 12706−12714.
7. Reddy, Y. V., Ding, Q., Lees-Miller, S. P., Meek, K., and Ramsden, D. A. (2004) Non-homologous end joining requires that the DNA-PK complex undergo an autophosphorylation-dependent rearrangement at DNA ends, *J. Biol. Chem. 279*, 39408−39413.
8. Block, W. D., Yu, Y., Merkle, D., Gifford, J. L., Ding, Q., Meek, K., and Lees-Miller, S. P. (2004) Autophosphorylation-dependent remodeling of the DNA-dependent protein kinase catalytic subunit regulates ligation of DNA ends, *Nucleic Acids Res. 32*, 4351−4357.
9. Ma, Y., Pannicke, U., Schwarz, K., and Lieber, M. R. (2002) Hairpin opening and overhang processing by an Artemis/DNA-dependent protein kinase complex in nonhomologous end joining and V(D)J recombination, *Cell 108*, 781−794.
10. Douglas, P., Sapkota, G. P., Morrice, N., Yu, Y., Goodarzi, A. A., Merkle, D., Meek, K., Alessi, D. R., and Lees-Miller, S. P. (2002) Identification of in vitro and in vivo phosphorylation sites in the catalytic subunit of the DNA-dependent protein kinase, *Biochem. J. 368*, 243−251.
11. Chan, D. W., Chen, B. P., Prithivirajsingh, S., Kurimasa, A., Story, M. D., Qin, J., and Chen, D. J. (2002) Autophosphorylation of the DNA-dependent protein kinase catalytic subunit is required for rejoining of DNA double-strand breaks, *Genes Dev. 16*, 2333−2338.
12. Soubeyrand, S., Pope, L., Pakuts, B., and Hache, R. J. (2003) Threonines 2638/2647 in DNA-PK are essential for cellular resistance to ionizing radiation, *Cancer Res. 63*, 1198−1201.
13. Ding, Q., Reddy, Y. V., Wang, W., Woods, T., Douglas, P., Ramsden, D. A., Lees-Miller, S. P., and Meek, K. (2003) Autophosphorylation of the catalytic subunit of the DNA-dependent protein kinase is required for efficient end processing during DNA double-strand break repair, *Mol. Cell. Biol. 23*, 5836−5848.
14. Meek, K., Gupta, S., Ramsden, D. A., and Lees-Miller, S. P. (2004) The DNA-dependent protein kinase: The director at the end, *Immunol. Rev. 200*, 132−141.
15. Kim, S. A., Heinze, K. G., Bacia, K. A., Waxham, M. N., and Schwille, P. (2005) Two-photon cross-correlation analysis of intracellular reactions with variable stoichiometry, *Biophys. J. 88*, 4319−4336.
16. Merkle, D., Lees-Miller, S. P., and Cramb, D. T. (2004) Structure and dynamics of lipoplex formation examined using two-photon fluorescence cross-correlation spectroscopy, *Biochemistry 43*, 7263−7272.
17. Weterings, E., Verkaik, N. S., Bruggenwirth, H. T., Hoeijmakers, J. H., and van Gent, D. C. (2003) The role of DNA dependent protein kinase in synapsis of DNA ends, *Nucleic Acids Res. 31*, 7238−7246.
18. Goodarzi, A. A., and Lees-Miller, S. P. (2004) Biochemical characterization of the ataxia-telangiectasia mutated (ATM) protein from human cells, *DNA Repair 3*, 753−767.
19. Sambrook, J., Fritsch, E. F., and Maniatis, T. (1989) *Molecular Cloning: A Laboratory Manual*, 2nd ed., Cold Spring Harbor Laboratory Press, Plainview, NY.
20. Ting, N. S., Kao, P. N., Chan, D. W., Lintott, L. G., and Lees-Miller, S. P. (1998) DNA-dependent protein kinase interacts with antigen receptor response element binding proteins NF90 and NF45, *J. Biol. Chem. 273*, 2136−2145.
21. Cary, R. B., Peterson, S. R., Wang, J., Bear, D. G., Bradbury, E. M., and Chen, D. J. (1997) DNA looping by Ku and the DNA-dependent protein kinase, *Proc. Natl. Acad. Sci. U.S.A. 94*, 4267−4272.
22. Yaneva, M., Kowalewski, T., and Lieber, M. R. (1997) Interaction of DNA-dependent protein kinase with DNA and with Ku: Biochemical and atomic-force microscopy studies, *EMBO J. 16*, 5098−5112.

BI0524060